

Confronting Kähler moduli inflation with CMB data

Sukannya Bhattacharya,^{*} Koushik Dutta,[†] and Mayukh Raj Gangopadhyay[‡]

*Theory Division, Saha Institute of Nuclear Physics,
HBNI,1/AF Bidhannagar, Kolkata- 700064, India*

Anshuman Maharana[§]

Harish Chandra Research Institute, HBNI, Chattnag Road, Jhansi, Allahabad - 211019, India.

In models of inflation obtained from string compactification, moduli vacuum misalignment leads to an epoch in the post-inflationary history of the universe when the energy density is dominated by cold moduli particles. This effect leads to a modification in the number of e -foldings (N_{pivot}) between horizon exit of the CMB modes and the end of inflation. Taking Kähler moduli inflation as a prototype, the shift in e -foldings turns out to be a function of the model parameters which also determines the inflationary observables. We analyse this scenario numerically using publicly available MODECHORD and COSMOMC with the latest *Planck+BICEP2/Keck array* data to constrain the model parameters and N_{pivot} . In light of the present and future precision data, the results show the importance of careful consideration of any post-inflationary non-standard epoch, as well as of the effects of reheating.

I. INTRODUCTION

The inflationary paradigm has provided an explanation for the observed spectrum and inhomogeneities in the Cosmic Microwave Background (CMB). Intense efforts are on to probe the CMB for tensor modes and non-Gaussianity. Observations of these will provide further credence to the theory. At the same time, programs to measure the spectral tilt of scalar modes (n_s) with greater accuracy are being planned. The ground based CMB-S4 experiment [1], the LiteBIRD satellite [2], and the CORE satellite [3], if approved, can significantly reduce the uncertainty in the measurement of the spectral tilt (projected uncertainty $\sigma(n_s) \sim 0.002$ at the $1\text{-}\sigma$ level). In this light, it is important to develop tools to extract accurate predictions for inflationary models.

The most commonly adopted method to constrain models of inflation is to express the primordial perturbations in terms of empirical parameters such as A_s (the strength of the power spectrum), n_s (the scalar tilt), r (the tensor to scalar ratio), f_{nl} (parametrising the non-Gaussianity) etc. The most likely values of the empirical parameters are determined by evolving the initial fluctuations (as expressed in terms of these parameters) and then comparing with the observed CMB fluctuations. Given a model of inflation, its theoretical prediction for the empirical parameters are computed as a function of model parameters, and a model is considered successful if the predicted values match the constraints on the empirical parameters from the observations. This indeed is the general procedure followed by the Planck collaboration to obtain constraints on several inflation models[4].

In this methodology, it is important to remember that the observables need to be calculated at certain e -folds back (N_{pivot}) from the end of inflation when CMB modes go outside the horizon, and N_{pivot} crucially depends on the post-inflationary cosmic history including the epoch of reheating, see for e.g [5].

If one is interested in confronting a particular model of inflation with data, then a robust approach can be taken, as developed in [6–8]. One takes the coefficients of the inflaton potential and the parametrisation of the reheating epoch as the ‘model inputs’. Observational predictions are examined directly in terms of the coefficients of the potential; estimates and errors for the coefficients of the potential are directly obtained. One of the ways, this can be achieved is by making use of MODECHORD¹[8] which provides a numerical evaluation of the inflationary perturbation spectrum (even without relying on the slow-roll approximation) taking the potential coefficients as input; which is then used as a plug-in for CAMB[9] and COSMOMC[10]. The parameters are then estimated using a nested sampling method[11]. The importance of reheating effects in constraining inflation models using current cosmological data was first discussed in [7], and was subsequently applied to the WMAP data in [12] and to the Planck data in [13].

The slow-roll conditions require the inflationary potential to be flat in Planck units. Any inflation model is sensitive to ultraviolet degrees of freedom, and therefore, inflation models should be embedded in ultraviolet complete theories. String theory being our best hope for an ultraviolet complete theory, inflationary models obtained from string theory deserve to be analysed in detail. This is best achieved by following the approach of [8]. Inflationary model building has been extensively studied in string theory (see e.g [14]).

^{*} sukannya.bhattacharya@saha.ac.in

[†] koushik.dutta@saha.ac.in

[‡] mayukh.raj@saha.ac.in

[§] anshumanmaharana@hri.res.in

¹ MODECHORD is publicly available at www.modecode.org

There is also a more pragmatic reason to analyse models obtained from string theory using this approach. String compactifications typically have moduli fields, which are massless scalars with interactions of gravitational strength. A generic feature of models of inflation constructed in string theory (and supergravity) is vacuum misalignment of moduli. This leads to an epoch in the post-inflationary history in which the energy density of the universe is dominated by cold moduli particles (see e.g. [15] for a recent review). The presence of such an epoch changes the number of e-foldings of the universe between horizon exit of the pivot mode and the end of inflation (N_{pivot}). Since the primordial perturbations are determined by local properties of the inflaton potential at the time of horizon exit, N_{pivot} has an effect on inflationary predictions. Recent work has shown that it is important to incorporate this effect while confronting string models with precision cosmological data [16, 17]; an accurate determination of N_{pivot} is essential. Furthermore, N_{pivot} has dependence on the model parameters that also determine inflationary observables. Given this, a complete numerical methodology using MODECHORD+COSMOMC [8, 10] is carried out in this work. In this paper, we will take Kähler moduli inflation [18], [19] as a prototype and analyse it using MODECHORD. Vacuum misalignment in the model was studied in [16], where the effect of this epoch on N_{pivot} was determined. We note that Kähler moduli inflation in light of Bayesian model selection was discussed in [20–22], their key difference between the present analysis and that of [20–22] is incorporation the effects of the fact that the duration of the epoch of modulus domination in the post-inflationary history depends on the model parameters.

This paper is organised as follows. In the next section, we first review some basic aspects of Kähler moduli inflation relevant for us. We then mention the duration of modulus dominated epoch at the end of inflation N_{mod} for the model. N_{mod} shifts the N_{pivot} from its usual number. In Sec. III we discuss the methodology for analysing the model parameters and how the required modification in N_{pivot} can be implemented in MODECHORD. In Sec. IV, we analyse and discuss the results for Generalised Reheating (GRH) scenario where N_{pivot} is varied between 20 and the number corresponding to the instantaneous reheating case. This analysis is independent of average equation of state parameter w_{re} during reheating. The case for specific values of w_{re} with the requirement of $T_{\text{re}} > T_{BBN}$ is analysed in Sec. V. We conclude in Sec. VI.

II. A BRIEF REVIEW OF KÄHLER MODULI INFLATION

We begin by briefly reviewing Kähler moduli inflation, the reader should consult [18] for further details. Kähler moduli inflation is set in the Large Volume Scenario (LVS) for moduli stabilisation [23, 24] of IIB flux

compactifications [25]. The complex structure moduli of the underlying Calabi-Yau are stabilised by fluxes. The simplest models of LVS are the ones in which the volume of the Calabi-Yau takes the Swiss-cheese form: $\mathcal{V} = \alpha \left(\tau_1^{3/2} - \sum_{i=2}^n \lambda_i \tau_i^{3/2} \right)$ [23, 24]. Note that the overall volume is set by τ_1 ; the moduli τ_2, \dots, τ_n are blow-up modes and correspond to the size of the holes in the compactification. Incorporating the non-perturbative effects in the superpotential, the leading α' correction to the Kähler potential and an uplift term (so that a nearly Minkowski vacuum can be obtained), the potential for the scalars in the regime $\mathcal{V} \gg 1$ and $\tau_1 \gg \tau_i$ (for $i > 1$) is

$$V_{\text{LVS}} = \sum_{i=2}^n \frac{8(a_i A_i)^2 \sqrt{\tau_i}}{3\mathcal{V}\lambda_i} e^{-2a_i \tau_i} - \sum_{i=2}^n \frac{4a_i A_i W_0}{\mathcal{V}^2} \tau_i e^{-a_i \tau_i} + \frac{3\hat{\xi} W_0^2}{4\mathcal{V}^3} + \frac{D}{\mathcal{V}^\gamma}. \quad (1)$$

Here A_i, a_i are the pre-factors and coefficients in the exponents of the non-perturbative terms in the superpotential and W_0 is the vacuum expectation value of flux superpotential. The uplift term is $V_{\text{up}} = \frac{D}{\mathcal{V}^\gamma}$ with $D > 0$, $1 \leq \gamma \leq 3$ (see [26–30] for mechanisms that can lead to such a term).

In Kähler moduli inflation, one of the blow-up moduli (τ_n) acts as the inflaton. For simplicity, we will focus on Calabi-Yau's of the Swiss Cheese form (although the analysis can be carried out in more general settings, [31]). Inflation takes place in region $e^{a_n \tau_n} \gg \mathcal{V}^2$, here the potential is well approximated by:

$$V_{\text{inf}} = \sum_{i=2}^{n-1} \frac{8(a_i A_i)^2 \sqrt{\tau_i}}{3\mathcal{V}\lambda_i} e^{-2a_i \tau_i} - \sum_{i=2}^{n-1} \frac{4a_i A_i W_0}{\mathcal{V}^2} \tau_i e^{-a_i \tau_i} + \frac{3\hat{\xi} W_0^2}{4\mathcal{V}^3} + \frac{D}{\mathcal{V}^\gamma} - \frac{4a_n A_n W_0}{\mathcal{V}^2} \tau_n e^{-a_n \tau_n}. \quad (2)$$

It is exponentially flat in the inflaton direction (τ_n). The other directions (\mathcal{V}, τ_i with $i = 2, \dots, n-1$) in field space are heavy during inflation. Integrating out the heavy directions and canonically normalising the inflaton (we denote the canonically normalised field by σ), one finds its potential (in Planck units) to be

$$V = \frac{g_s}{8\pi} \left(V_0 - \frac{4W_0 a_n A_n}{\mathcal{V}_{\text{in}}^2} \left(\frac{3\mathcal{V}_{\text{in}}}{4\lambda_n} \right)^{2/3} \sigma^{4/3} \right) \times \exp \left[-a_n \left(\frac{3\mathcal{V}_{\text{in}}}{4\lambda_n} \right)^{2/3} \sigma^{4/3} \right], \quad (3)$$

where

$$\frac{\sigma}{M_{\text{pl}}} = \sqrt{\frac{4\lambda_n}{3\mathcal{V}_{\text{in}}}} \tau_n^{\frac{3}{4}} \quad \text{with} \quad V_0 = \frac{\beta W_0^2}{\mathcal{V}_{\text{in}}^3}. \quad (4)$$

\mathcal{V}_{in} is the value of the volume during inflation and $\beta = \frac{3}{2} \lambda_n a_n^{-3/2} (\ln \mathcal{V})^{3/2}$. Phenomenological considerations put

the volume at $\mathcal{V}_{\text{in}} \approx 10^5 - 10^7$, and we will discuss cosmological constraints on it in the next section. We note that ‘global embedding’ of the model (realisation in a compact Calabi-Yau with a semi-realistic Standard Model sector) was carried out in [32].

Vacuum misalignment and the resulting post-inflationary moduli dynamics in this model was studied in detail in [16], here we summarise its conclusions. During inflation, the volume modulus gets displaced from its global minimum. The displacement of the canonically normalised field in Planck units is:

$$Y = 2R \left(\frac{\hat{\xi}}{2P} \right)^{2/3}$$

with

$$R = \frac{\lambda_n a_n^{-3/2}}{\left(\sum_i^n \lambda_i a_i^{-3/2} \right)}, \quad P = \sum_i^n \lambda_i a_i^{-3/2},$$

and $\hat{\xi} = \frac{\chi}{2(2\pi)^3 g_s^{3/2}}$,

where χ is the Euler number of the Calabi-Yau and g_s is the vacuum expectation value of the dilaton. For typical values of the microscopic parameters, $Y \approx 0.1$ which is consistent with effective field theory expectations. This leads to an epoch in the post-inflationary history in which the energy density is dominated by cold particles of the volume modulus. The number of e -foldings that the universe undergoes in this epoch is [16]

$$N_{\text{mod}} = \frac{2}{3} \ln \left(\frac{16\pi a_n^{2/3} \mathcal{V}^{5/2} Y^4}{10\lambda_n (\ln \mathcal{V})^{1/2}} \right). \quad (5)$$

The presence of this epoch reduces the number of e -foldings between horizon exit of the pivot mode and the end of inflation by an amount $\frac{1}{4}N_{\text{mod}}$. The spectral index can be calculated by using the usual slow-roll formula $n_s \approx 1 - 2/N_{\text{pivot}}$, but at the reduced value of N_{pivot} . For typical values of the volume $\mathcal{V} \sim 10^5 - 10^6$ and other parameters in this model, N_{mod} can be calculated. In Kähler moduli inflation, the inflaton decays to relativistic d.o.f at the end of inflation, the energy density of these relativistic degrees of freedom becomes subdominant quickly in comparison with the energy density of the oscillating volume modulus (which arises as a result of vacuum misalignment). For typical values of the model parameters, this epoch of between inflation and modulus domination has a small duration and hence a negligible effect on N_{pivot} [16]. We therefore neglect this epoch in our analysis. After the decay of the volume modulus, the universe has standard thermal history.

III. METHODOLOGY OF ANALYSIS

The analysis is dependent on the exact definition of the number of e -foldings N_{pivot} . The correctly measured

number of e -foldings at the horizon exit is crucial to constrain models of inflation with an additional epoch of post-inflationary moduli domination. This analysis is devised to see how the change in predicted number of e -foldings during inflation due to the secondary moduli dominated epoch effects the observables and therefore constrains the model parameters. But, even though the modulus dominated epoch is considered carefully, there is inherent uncertainties with the exact value of N_{pivot} due to our poor knowledge about the details of reheating/preheating at the end of modulus domination. With better understanding of several couplings between the inflation/modulus with Standard Model d.o.f, in future we will possibly find the total duration of the thermalization process N_{re} with its average equation of state parameter w_{re} . Until this is available, it is practical to consider the reheating parameters w_{re} and N_{re} as variables when analysing the model in light of the recent CMB data.

The analysis is carried out using the publicly available CosmoMC [10] and MODECHORD [8] plugged together through Multinest [11]. Given a typical model of inflation, MODECHORD numerically computes the primordial scalar and tensor power spectra. These primordial spectra are fed to the CAMB in the CosmoMC package with the help of the plug-in software Multinest to evolve through transfer functions. The theoretically calculated perturbations at the CMB redshift is then compared to the observed fluctuations using CosmoMC. CosmoMC is a multi-dimensional Markov Chain Monte Carlo simulator which in this case compares the C_l values computed numerically for the given inflationary model with the observed C_l values by Planck and BICEP-Keck array [33–35]. In general, all the model parameters of inflation and late time cosmological parameters (e.g. Ω_b , Ω_c , θ and τ) are variables in this ModeChord+CosmoMC set up. In addition, number of e -folds of inflation can also be set as a variable due to our lack of knowledge of the (p)reheating epoch. In this work, we have varied all the late time cosmological parameters in the six-parameter Λ CDM model as well as the number of e -folds during inflation. The ranges of the inflationary model parameters which are varied in the simulation are chosen carefully and particularly the ranges for the reheating parameters are explained in the following paragraphs.

For the generic inflation scenario with instantaneous reheating (IRH) where the universe thermalizes instantly after inflation and makes quick transition to the radiation dominated epoch, the number of e -foldings at the pivot scale is given by [8]:

$$N_{\text{pivot}}^{\text{IRH}} = 55.75 - \log \left[\frac{10^{16} \text{Gev}}{V_{\text{pivot}}^{1/4}} \right] + \log \left[\frac{V_{\text{pivot}}^{1/4}}{V_{\text{end}}^{1/4}} \right]. \quad (6)$$

Here, V_{pivot} is the value of the inflation potential at which the pivot scale leaves the horizon and V_{end} is the potential at the end of inflation. From the observational upper limit of the strength of the gravitational wave ($r < 0.11$ [4]), the second term in the above equation is negative,

whereas the third term is positive definite, but it can be very small for observationally favoured flat inflaton potential. In the usual implementation of MODECHORD, the cosmological perturbations are evaluated without assuming slow-roll conditions, and the best-fit potential parameters can be estimated using CosmoMC. But this also requires that the uncertainties associated with reheating are accounted for, and this can be done by varying N_{pivot} between $20 < N_{\text{pivot}} < N_{\text{pivot}}^{\text{IRH}}$. This is termed as the general reheating (GRH) scenario [8]. The upper limit is motivated from the assumption that the average dilution of energy density during the reheating epoch is not faster than radiation, i.e. $w_{\text{re}} \leq 1/3$. The lower limit comes from the requirement that at the end of inflation, all the cosmologically relevant scales are well outside of the horizon. The shortcoming of this approach is that the reheating scenarios with $w_{\text{re}} > 1/3$ are not considered; the possibility that N_{pivot} can be above N_{IRH} is excluded in this analysis.

If there is an epoch of moduli domination in the post-inflationary history, then Eq. 6 gets modified. For Kähler moduli inflation N_{mod} is given by Eq. 5, and in this case $N_{\text{pivot}}^{\text{IRH}}$ is:

$$N_{\text{pivot}}^{\text{IRH}} = 55.75 - \log \left[\frac{10^{16} \text{Gev}}{V_{\text{pivot}}^{1/4}} \right] + \log \left[\frac{V_{\text{pivot}}^{1/4}}{V_{\text{end}}^{1/4}} \right] - \frac{1}{6} \ln \left(\frac{16\pi a_n^{2/3} \mathcal{V}^{5/2} Y^4}{10\lambda_n (\ln \mathcal{V})^{1/2}} \right). \quad (7)$$

Note the additional dependence on the model parameters that arises from the last term in Eq. (7). In our analysis for $-1/3 < w_{\text{re}} \leq 1/3$, we will vary N_{pivot} between 20 and $N_{\text{pivot}}^{\text{IRH}}$ given by Eq. (7).

In general, N_{pivot} is determined by $N_{\text{pivot}}^{\text{IRH}}$ (as determined by equation (7)), w_{re} and N_{re} :

$$N_{\text{pivot}} = N_{\text{pivot}}^{\text{IRH}} - \frac{1}{4}(1 - 3w_{\text{re}})N_{\text{re}}. \quad (8)$$

The most general reheating case for the modulus can be treated with considering $-1/3 < w_{\text{re}} < 1$, where the upper bound comes from the positivity conditions in general relativity. The GRH analysis as previously discussed in this section implicitly scans the region $-1/3 < w_{\text{re}} < 1/3$, where N_{pivot} becomes maximum when the contribution of the last term in Eq. 8 is minimum (vanishes) for $w_{\text{re}} = 1/3$, i.e. instantaneous reheating. This allows us to put $N_{\text{pivot}}^{\text{IRH}}$ as the upper bound for N_{pivot} while varying it inside ModeChord+CosmoMC for $-1/3 < w_{\text{re}} < 1/3$. But, in the region $1/3 < w_{\text{re}} < 1$, the contribution from the last term in Eq. 8 becomes positive which increases the value of N_{pivot} beyond $N_{\text{pivot}}^{\text{IRH}}$. Therefore, we cannot use the previous prior range for N_{pivot} to analyse for $1/3 < w_{\text{re}} < 1$.

We note that for the case $1/3 < w_{\text{re}} < 1$ the last term in Eq. 8 contributes maximum when w_{re} is maximum ($w_{\text{re}} = 1$) and N_{re} is maximum also. Now, N_{re}

becomes maximum for the lowest allowed reheating temperature that must be above the Big Bang Nucleosynthesis (BBN) bound, namely $T_{\text{re}} > T_{\text{BBN}} = 5.1 \text{ MeV}$ [36]. Therefore, we have examined the general reheating scenario by simulating with ModeChord+CosmoMC for a few fixed values of w_{re} with the minimum reheating temperature with $T_{\text{re}} = T_{\text{BBN}}$. For particular values of w_{re} in the range $1/3 < w_{\text{re}} < 1$, we set the upper bound on N_{pivot} as $N_{\text{pivot}}^{\text{IRH}} - \frac{1}{4}(1 - 3w_{\text{re}})N_{\text{re}}^{\text{max}}$, where $N_{\text{re}}^{\text{max}}$ is N_{re} derived with $T_{\text{re}} = T_{\text{BBN}} = 5.1 \text{ MeV}$ for a fixed value of w_{re} . In Sec. V, we will discuss in detail how we find $N_{\text{re}}^{\text{max}}$ for $T_{\text{re}} = T_{\text{BBN}}$. Our methodology here differs from the previous analyses done in Ref. [20–22] in terms of parametrisation of the reheating epoch in terms of the underlying model parameters and statistical techniques used for parameter estimation.

In summary, we incorporate the effects of reheating using two different methods (and carry out the analysis to obtain the preferred value of the model parameters using both the methods)

- (i) Analysis using the GRH scenario, and in this case, we vary N_{pivot} between $N_{\text{pivot}}^{\text{IRH}}$ as given by (7) and 20.
- (ii) Analysis for specific values of w_{re} . In this case, N_{pivot} varies between $N_{\text{pivot}}^{\text{IRH}}$ and the $\hat{N}_{w_{\text{re}}}$, with $\hat{N}_{w_{\text{re}}}$, determined by the requirement of reheating temperature being above the temperature needed for successful big bang nucleosynthesis.

IV. ANALYSIS AND RESULTS IN THE GRH SCENARIO

As described above, in the GRH scenario reheating uncertainties are accounted for by varying N_{pivot} between minimum value of 20 and $N_{\text{pivot}}^{\text{IRH}}$ given by Eq. (7). The model parameters (as defined in Sec. II) are varied in the following ranges: W_0 : 0.001 to 130, $\log_{10} \mathcal{V}$: 5 to 8 and A_n : 1.80 to 1.95. We take $g_s = 0.06$ (as required for a local realisation of the Standard Model from D3 branes), $\lambda_n = 1$ and $a_n = 2\pi$. We keep these parameters fixed as the observables depend mildly on these parameters, and these choices of the parameters are well motivated from the theoretical stand point. Note that among all these parameters $\log_{10} \mathcal{V}$ also determines the duration of modulus domination epoch, and therefore also affects N_{pivot} . The likelihoods used are *Planck TT+TE+EE*, *Planck lowP*, estimated using commander, *Planck lensing* and *Planck+BICEP2/Keck array* joint analysis likelihood [33–35].

In Fig. 1 and Fig. 2, we show the $1\text{-}\sigma$ and $2\text{-}\sigma$ bounds on the model parameters. While Fig. 1 shows the marginalised constraint on the parameters W_0 and $\log_{10} \mathcal{V}$, Fig. 2 shows the marginalised constraint on W_0 and A_n . These plots represent the most favourable region of the model parameters when N_{pivot} is varied between

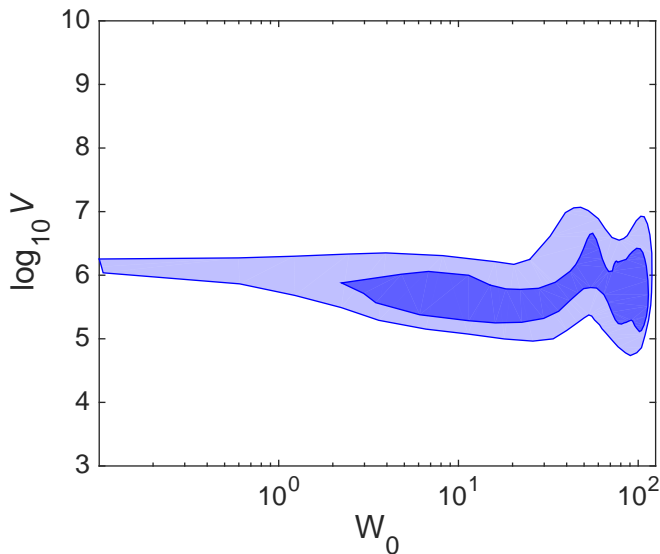


FIG. 1. Favoured regions in the $W_0 - \log_{10} \mathcal{V}$ plane. The $1-\sigma$ region is shaded as dark blue, the $2-\sigma$ region is shaded as light blue.

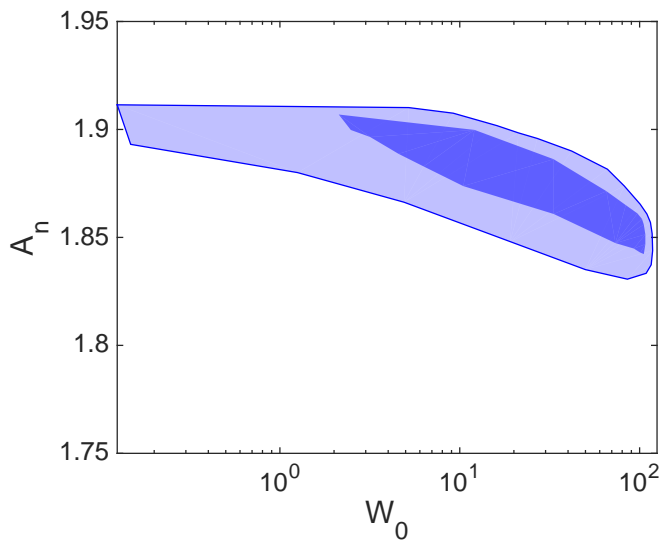


FIG. 2. Favoured regions in the $W_0 - A_n$ plane. The $1-\sigma$ region is shaded as dark blue, the $2-\sigma$ region is shaded as light blue.

20 to $N_{\text{pivot}}^{\text{IRH}}$ for this given model. The marginalised central value and the $1-\sigma$ errors are quoted in the Table I. Note that W_0 is not constrained as tightly as the other two parameters. The central value of the spectral index $n_s \sim 0.953$ obtained from the simulation corresponds to number of e -folds $N_{\text{pivot}} = 43$. This is in keeping with the theoretical expectation with $n_s \approx 1 - 2/N_{\text{pivot}}$, derived under the slow-roll approximations.

The favoured region in the n_s-r plane is presented in Fig.3. Note that the results are in agreement with earlier analytic treatments [16, 32]. But, here we would like to emphasise the difference also. In [16], the shift

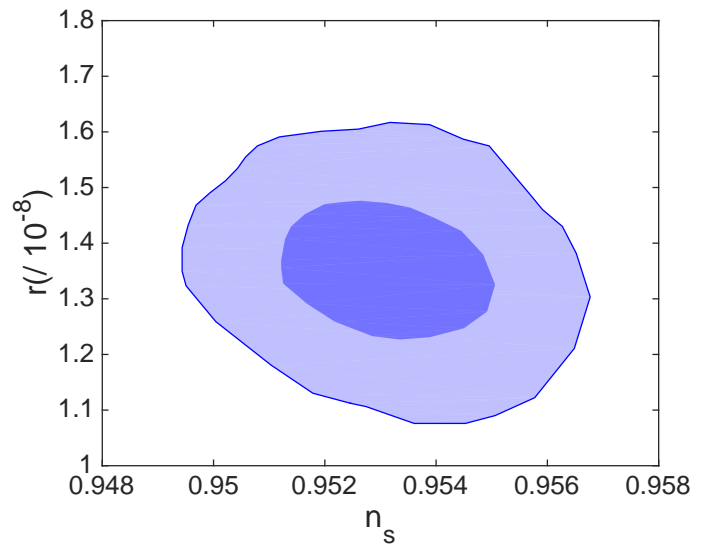


FIG. 3. Favoured region in the n_s-r plane. The $1-\sigma$ region is shaded as dark blue, the $2-\sigma$ region is shaded as light blue.

TABLE I. Constraints on the model parameters and the cosmological parameters. Data combination used: *Planck TT + TE + EE + lowP + lensing + BKPlanck14*.

Parameters	Central Value	1σ
W_0	57	46
$\log_{10} \mathcal{V}$	5.9	0.3
A_n	1.87	0.04
n_s	0.953	0.002
$r/10^{-8}$	1.34	0.1
N_{pivot}	43	2

in the N_{pivot} was calculated by using Eq. (5) where $\mathcal{V} \sim 10^5 - 10^6$, fixed by the amplitude of scalar perturbations for typical microscopic parameters. Effectively, the spectral index was calculated at $N_{\text{pivot}} \sim 45$ with $n_s \sim 0.955$. But now, we have kept both \mathcal{V} and N_{pivot} as variables under the generalised reheating scheme, and find preferred values comparing with the data. We present the distribution of N_{pivot} (marginalised over all other parameters) in Fig. 4. We see that as an effect of precision analysis to determine exact values of the model parameters, the central value of N_{pivot} shifts to 43 from 45 as found in [16].

Note that the lower $2-\sigma$ bound on N_{pivot} is 39, which is well above 20 and closer to $N_{\text{pivot}}^{\text{IRH}} = 45$. As is evident from the best fit value of $n_s = 0.953 \pm 0.002$, the model is outside of the PLANCK ($\Lambda\text{CDM}+r$) $2-\sigma$ lower limit [4]². Our analysis also provides a χ^2 value for the model, and we find that with equal number of parameters to be varied, there is a deterioration of the fit in this case by $\Delta\chi^2 \simeq 13$ with respect to the $\Lambda\text{CDM}+r$ model for the

² Although the model can be consistent when the effects of dark radiation are considered [32, 37].

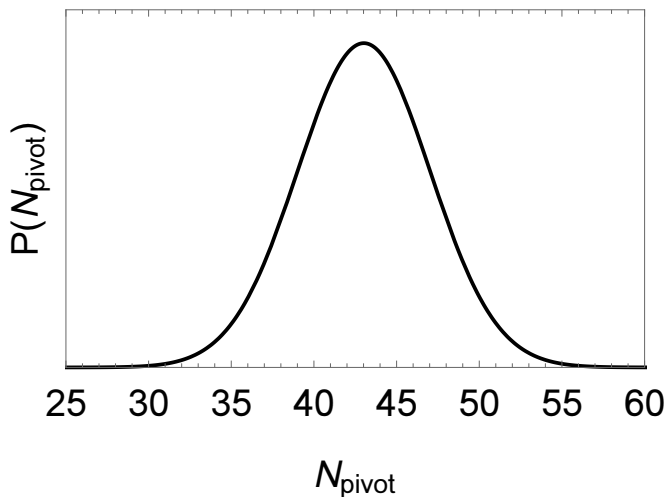


FIG. 4. 1-D probability distribution of the number of e-foldings N_{pivot} .

same combination of the CMB data.

V. ANALYSIS AND RESULTS FOR SPECIFIC VALUES OF w_{re}

In this section we carry out our analysis by making specific choices for w_{re} ($w_{\text{re}} = 0, 2/3, 1$). As discussed earlier, we will determine the range for variation of N_{pivot} by using the expression for $N_{\text{pivot}}^{\text{IRH}}$ and the requirement of successful nucleosynthesis. Before going on to analyse the model for various value of w_{re} , let us first describe how we determine this range.

The Hubble parameter at the end of the reheating epoch (after the modulus decay) is given by [16]

$$H(\hat{t}) = \frac{M_{\text{pl}} W_0^3}{16\pi \mathcal{V}^{9/2} (\ln \mathcal{V})^{3/2}} \exp\left(-\frac{3}{2}(1+w_{\text{re}})N_{\text{re}}\right). \quad (9)$$

Moreover, the reheating temperature is given by $3M_{\text{pl}}^2 H^2(\hat{t}) = \rho(\hat{t}) \approx \frac{\pi^2}{30} g_* T_{\text{re}}^4$, where g_* is the effective number of degrees of freedom of the Standard Model sector. Thus N_{re} can be expressed in terms of the model parameters, the effective equation of state during reheating and the reheating temperature:

$$N_{\text{re}} = -\frac{2}{3} \left(\frac{1}{1+w_{\text{re}}} \right) \ln \left[\frac{16\pi^2 g_*^{1/2} \mathcal{V}^{9/2} (\ln \mathcal{V})^{3/2} T_{\text{re}}^2}{\sqrt{90} M_{\text{pl}}^2 W_0^3} \right]. \quad (10)$$

Successful nucleosynthesis requires $T_{\text{re}} > T_{\text{BBN}} = 5.1$ MeV [36]. Plugging this condition in (10) we find an upper bound for N_{re} . We will denote this value by $N_{\text{re}}^{\text{max}}$ (note that this quantity depends on w_{re}). Now, in general, N_{pivot} is determined by Eq. (8). Since for a given value of w_{re} , N_{re} is bounded to lie in the range $(0, N_{\text{re}}^{\text{max}})$, the allowed range for N_{pivot} is between N^{IRH} and $N^{\text{IRH}} - \frac{1}{4}(1-3w_{\text{re}})N_{\text{re}}^{\text{max}}$. Note that $N^{\text{IRH}} - \frac{1}{4}(1-$

$3w_{\text{re}})N_{\text{re}}^{\text{max}}$ is greater than N^{IRH} for $w_{\text{re}} > 1/3$, thus for $w_{\text{re}} > 1/3$, N_{pivot} lies in the interval of

$$(N^{\text{IRH}}, N^{\text{IRH}} - \frac{1}{4}(1-3w_{\text{re}})N_{\text{re}}^{\text{max}}).$$

On the other hand for $w_{\text{re}} < 1/3$, N_{pivot} lies in the interval of $(N^{\text{IRH}} - \frac{1}{4}(1-3w_{\text{re}})N_{\text{re}}^{\text{max}}, N^{\text{IRH}})$. Next, we carry out the analysis to obtain the preferred value of the model parameters for $w_{\text{re}} = 1, 2/3, 0$. N_{pivot} is taken to lie within N^{IRH} and $N^{\text{IRH}} - \frac{1}{4}(1-3w_{\text{re}})N_{\text{re}}^{\text{max}}$. For all the analyses below, we vary the model parameters W_0 , $\log_{10} \mathcal{V}$ and A_n in the prior ranges same as section III, i.e., $W_0 : 0.001$ to 130 , $\log_{10} \mathcal{V} : 5$ to 8 and $A_n : 1.80$ to 1.95 . The values of the fixed parameters g_s and a_n are also same as section III. For the case of $w_{\text{re}} = 2/3$, Fig. 5 and Fig. 6 are the 2-D marginalised plots for the model parameters, and for $w_{\text{re}} = 1$, the plots are similar looking.

For the sake of completeness, we also do the analysis in this mechanism for a single $w_{\text{re}} < 1/3$ case, $w_{\text{re}} = 0$. Here, the lower bound to N_{pivot} can be specified as $N_{\text{pivot}}^{\text{IRH}} - \frac{1}{4}(1-3w_{\text{re}})N_{\text{re}}^{\text{max}}$. Therefore, here, we vary N_{pivot} in the range $N_{\text{pivot}}^{\text{IRH}} - \frac{1}{4}(1-3w_{\text{re}})N_{\text{re}}^{\text{max}} < N_{\text{pivot}} < N_{\text{pivot}}^{\text{IRH}}$.

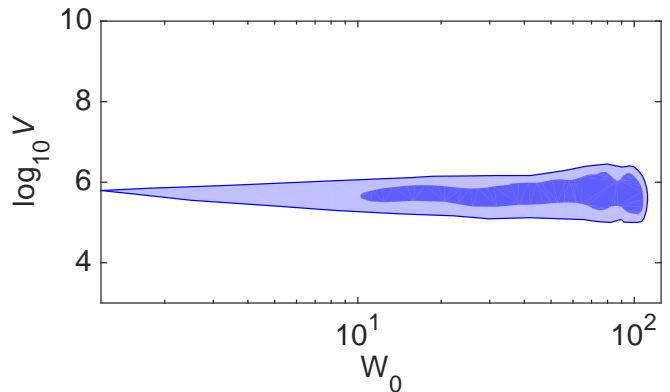


FIG. 5. Favoured regions in the $W_0 - \log_{10} \mathcal{V}$ plane for $w_{\text{re}} = 2/3$. The 1- σ region is shaded as dark blue, the 2- σ region is shaded as light blue.

The best-fit values and 1- σ errors for the above three cases $w_{\text{re}} = 2/3, 1, 0$ are quoted in Table II. The values of the model parameters are well within 1- σ of the values quoted in Table I in Section III. The 2-D marginalised plot in the $n_s - r$ plane is given in Fig. 7 for the above three cases. The 1-D marginalised posterior distribution for corresponding N_{pivot} are shown in Fig. 8.

From table II, the best-fit values of the the scalar spectral index (n_s) for the cases with $w_{\text{re}} > 1/3$ is greater than n_s for $w_{\text{re}} = 0$ and also greater than the value quoted in Table I for general $w_{\text{re}} < 1/3$ cases. Moreover, exotic reheating scenarios ($w_{\text{re}} > 1/3$) produce n_s values closer to the current marginalised mean values given by Planck 2015 ($\Lambda\text{CDM} + r$) [4] than for the $w_{\text{re}} < 1/3$ cases. For $w_{\text{re}} = 2/3$, the value of n_s is just at the lower 2- σ bound given by Planck, whereas for the $w_{\text{re}} = 1$ case,

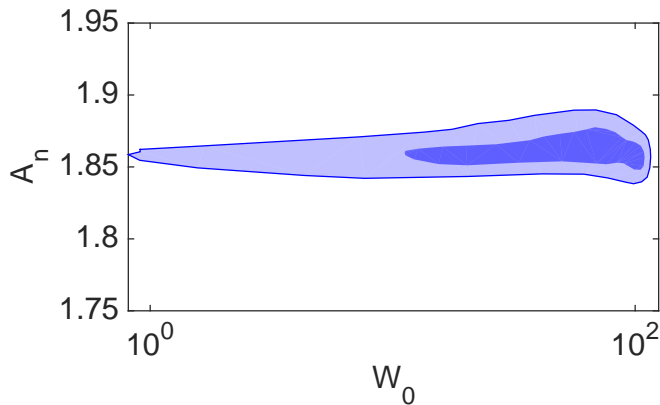


FIG. 6. Favoured regions in the $W_0 - A_n$ plane for $w_{\text{re}} = 2/3$. The $1\text{-}\sigma$ region is shaded as dark blue, the $2\text{-}\sigma$ region is shaded as light blue.

TABLE II. Constraints on the model parameters and cosmological parameters for $w_{\text{re}} = 2/3, 1, 0$. Data combination used: *Planck TT + TE + EE + lowP + lensing + BKPlanck14*.

	$w_{\text{re}} = 0$	$w_{\text{re}} = 2/3$	$w_{\text{re}} = 1$
Parameters	Best-fit $\pm 1\sigma$	Best-fit $\pm 1\sigma$	Best-fit $\pm 1\sigma$
W_0	56.9 ± 46.5	58 ± 45	59 ± 48
$\log_{10} \mathcal{V}$	5.9 ± 0.3	5.9 ± 0.3	5.9 ± 0.3
A_n	1.87 ± 0.04	1.867 ± 0.03	1.865 ± 0.05
n_s	0.9535 ± 0.002	0.9555 ± 0.003	0.9575 ± 0.003
$r/10^{-8}$	1.34 ± 0.1	1.33 ± 0.1	1.31 ± 0.1
N_{pivot}	43 ± 2.5	45.2 ± 2.25	47.7 ± 2

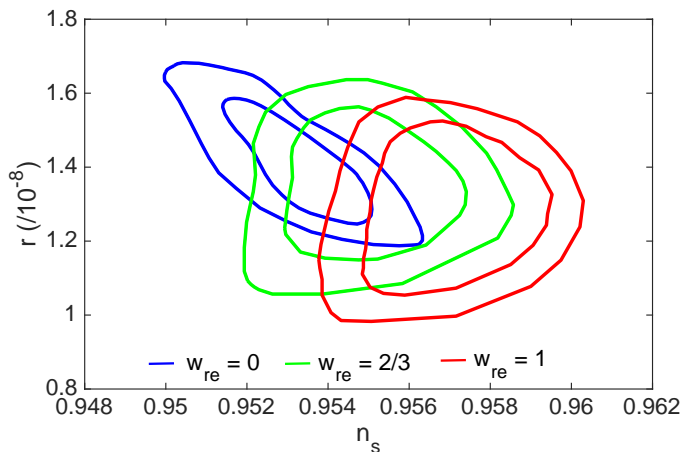


FIG. 7. $1\text{-}\sigma$ and $2\text{-}\sigma$ confidence levels in the $n_s - r$ plane for $w_{\text{re}} = 0$ (blue contours), $w_{\text{re}} = 2/3$ (green contours) and $w_{\text{re}} = 1$ (red contours).

n_s is inside the Planck $2\text{-}\sigma$ bound³. Projected sensitivity of n_s in future CMB experiments [1] are expected to resolve this situation with stronger constraints. If we look at the Fig. 7, we note that all possible reheating scenarios are consistent to each other at $2\text{-}\sigma$ level. But it is impor-

³ This is consistent to the analysis in Ref [38].

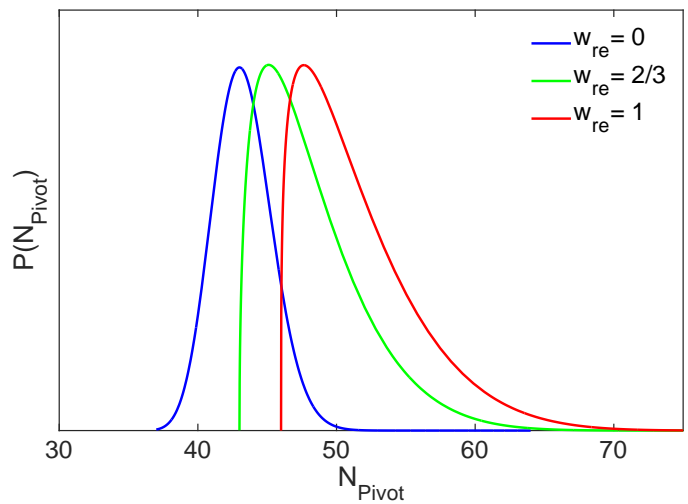


FIG. 8. 1-D posterior probability distribution of the number of e-foldings N_{pivot} for $w_{\text{re}} = 0$ (in blue), $w_{\text{re}} = 2/3$ (in green) and $w_{\text{re}} = 1$ (in red).

tant to appreciate that future observations are going to measure n_s with $\sigma(n_s) \sim 0.002$ at $1\text{-}\sigma$ level, and in that case, attempts to make meaningful statements about the value of the scalar spectral index automatically requires our better understanding regarding the reheating epoch. We also note that N_{pivot} has a larger value in the exotic reheating cases, which is expected from the positive contribution of the last term in Eq. 8. The tensor-to-scalar ratio r is of the same order ($\sim 10^{-8}$) in all of the above cases.

VI. CONCLUSIONS

In this paper, we have initiated the analysis of string models of inflation using MODECHORD. Given the ultra-violet sensitivity of inflation and the fact that so far the number of inflationary models that have been obtained from string theory is not large [14], it is natural to use MODECHORD when we try to confront them with data. As data becomes more and more precise N_{pivot} has to be determined very accurately. N_{pivot} itself can explicitly depend on the model parameters for string/supergravity models. Thus, analysis along the line of the present work will become more pertinent as cosmological observations become more precise. In this work, we constrain model parameters for Kähler moduli inflation, for which the ranges of observables are sensitive to future precision CMB measurements.

It is known in the literature that an additional post-inflationary era (like moduli domination in our case) is completely degenerate with the re-heating from the CMB point of view [12] unless the dynamics of the reheating

epoch is related to the model parameters⁴. But this is precisely what happens in the model at hand, the number of e-folds during reheating is known in terms of inflation model parameters which in turn also fixes inflationary observables (this is also the novel feature in the theoretical aspects our analysis of Kahler moduli inflation in comparison with [20–22]). We would like to emphasise that the relation between the modulus dominated epoch and the model parameters arose from embedding of the model and our knowledge of the low energy effective action the setting.

There are several interesting directions to pursue. The parameters in the inflationary potentials in string models themselves might have a statistical distribution, and one can try to incorporate the effect of this into the analysis. Another interesting direction is to understand degeneracies that can arise across the parameters and the model space. It will also be interesting to cross correlate with particle physics observables (see for e.g [41, 42]) and dark

radiation [37] in LVS. Note that the constraints of volume and W_0 will have direct implications for the supersymmetry breaking scale. The possibility of analysing multi-field models⁵ can be explored using MULTIMODECODE. [44]. Another exiting avenue is to develop a better understanding of the reheating epoch⁶ in these models so that associated uncertainties can be reduced. An recent development in this direction is the possibility that the number of e-foldings during the reheat epoch is bounded [46]. We hope to return to these questions in near future.

ACKNOWLEDGEMENTS

Both KD and AM are partially supported by Ramanujan Fellowships funded by SERB, DST, Govt. of India. SB is supported by a fellowship from CSIR, Govt of India. We sincerely thank the referee for the suggestions on on the initial version of the draft.

-
- [1] K. N. Abazajian *et al.* [CMB-S4 Collaboration], arXiv:1610.02743 [astro-ph.CO].
- [2] T. Matsumura *et al.*, *J. Low. Temp. Phys.* **176**, 733 (2014) doi:10.1007/s10909-013-0996-1 [arXiv:1311.2847 [astro-ph.IM]].
- [3] F. Finelli *et al.* [CORE Collaboration], arXiv:1612.08270 [astro-ph.CO].
- [4] Planck Collaboration, P. A. R. Ade *et al.*, *Astron. Astrophys.* **594** (2016) A20,
- [5] A. R. Liddle and S. M. Leach, *Phys. Rev. D* **68**, 103503 (2003) doi:10.1103/PhysRevD.68.103503 [astro-ph/0305263].
- [6] J. Martin, C. Ringeval, *JCAP* **0608** (2006) 009 doi: 10.1088/1475-7516/2006/08/009 [arXiv: astro-ph/0605367]
- [7] J. Martin and C. Ringeval, *Phys. Rev. D* **82**, 023511 (2010) doi:10.1103/PhysRevD.82.023511 [arXiv:1004.5525].
- [8] M. J. Mortonson, H. V. Peiris and R. Easther, *Phys. Rev. D* **83** (2011) 043505 doi:10.1103/PhysRevD.83.043505 [arXiv:1007.4205].
- [9] A. Lewis, A. Challinor and A. Lasenby, *Astrophys. J.*, 538, 473 (2000).
- [10] Antony Lewis and Sarah Bridle, *Phys. Rev. D* **66** (2002) [arXiv: astro-ph/0205436]
- [11] F. Feroz, M. P. Hobson and M. Bridges, *Mon. Not. Roy. Astron. Soc.* 398: 1601-1614,2009 DOI: 10.1111/j.1365-2966.2009.14548.x arXiv:0809.3437 [astro-ph] F. Feroz and M. P. Hobson, *Mon. Not. Roy. Astron. Soc.*, 384, 2, 449-463 (2008) DOI: 10.1111/j.1365-2966.2007.12353.x arXiv:0704.3704 [astro-ph] F. Feroz, M. P. Hobson, E. Cameron and A. N. Pettitt, arXiv:1306.2144 [astro-ph.IM]
- [12] J. Martin, C. Ringeval and R. Trotta, *Phys. Rev. D* **83**, 063524 (2011) doi:10.1103/PhysRevD.83.063524 [arXiv:1009.4157 [astro-ph.CO]].
- [13] J. Martin, C. Ringeval, R. Trotta and V. Vennin, *JCAP* **1403**, 039 (2014) doi:10.1088/1475-7516/2014/03/039 [arXiv:1312.3529 [astro-ph.CO]].
- [14] D. Baumann and L. McAllister, arXiv:1404.2601 [hep-th].
- [15] G. Kane, K. Sinha and S. Watson, *Int. J. Mod. Phys. D* **24**, no. 08, 1530022 (2015) doi:10.1142/S0218271815300220 [arXiv:1502.07746 [hep-th]].
- [16] M. Cicoli, K. Dutta, A. Maharana and F. Quevedo, *JCAP* **1608**, no. 08, 006 (2016) doi:10.1088/1475-7516/2016/08/006 [arXiv:1604.08512 [hep-th]].
- [17] K. Dutta and A. Maharana, *Phys. Rev. D* **91** (2015) no.4, 043503 doi:10.1103/PhysRevD.91.043503 [arXiv:1409.7037 [hep-ph]]. K. Das, K. Dutta and A. Maharana, *Phys. Lett. B* **751**, 195 (2015) doi:10.1016/j.physletb.2015.10.041 [arXiv:1506.05745 [hep-ph]].
- [18] J. P. Conlon and F. Quevedo, *JHEP* **0601** (2006) 146 [hep-th/0509012].
- [19] S. Lee and S. Nam, *Int. J. Mod. Phys. A* **26**, 1073 (2011) doi:10.1142/S0217751X1105155X [arXiv:1006.2876 [hep-th]].
- [20] J. Martin, C. Ringeval and V. Vennin, *Phys. Rev. Lett.* **114**, no. 8, 081303 (2015) doi:10.1103/PhysRevLett.114.081303 [arXiv:1410.7958 [astro-ph.CO]].
- [21] J. Martin, C. Ringeval and V. Vennin, *Phys. Dark Univ.* **5-6**, 75 (2014) doi:10.1016/j.dark.2014.01.003 [arXiv:1303.3787 [astro-ph.CO]].
- [22] J. Martin, C. Ringeval, V. Vennin, *Phys. Rev. D* **93** no.10, 103532 (2016) doi: 10.1103/PhysRevD.93.103532

⁴ The degeneracy can also be broken by the detection of primordial gravitational waves, see [39], [40]

⁵ For Kähler moduli inflation, the single field approximation is valid for a large class of initial conditions [43].

⁶ See [38, 45] for a phenomenological approach towards reheating for inflationary models in LVS.

- [arXiv:1603.02606 [astro-ph.CO]]
- [23] V. Balasubramanian, P. Berglund, J. P. Conlon, and F. Quevedo, *JHEP* **03** (2005) 007, [arXiv:hep-th/0502058].
- [24] J. P. Conlon, F. Quevedo and K. Suruliz, *JHEP* **0508** (2005) 007 [hep-th/0505076].
- [25] S. B. Giddings, S. Kachru and J. Polchinski, *Phys. Rev. D* **66** (2002) 106006 doi:10.1103/PhysRevD.66.106006 [hep-th/0105097].
- [26] S. Kachru, R. Kallosh, A. D. Linde and S. P. Trivedi, *Phys. Rev. D* **68** (2003) 046005 [hep-th/0301240].
- [27] M. Cicoli, A. Maharana, F. Quevedo and C. P. Burgess, *JHEP* **1206** (2012) 011 [arXiv:1203.1750 [hep-th]]; A. Retolaza and A. Uranga, arXiv:1512.06363 [hep-th].
- [28] C. P. Burgess, R. Kallosh and F. Quevedo, *JHEP* **0310**, 056 (2003) doi:10.1088/1126-6708/2003/10/056 [hep-th/0309187].
- [29] M. Cicoli, D. Klevers, S. Krippendorff, C. Mayrhofer, F. Quevedo and R. Valandro, *JHEP* **1405** (2014) 001 doi:10.1007/JHEP05(2014)001 [arXiv:1312.0014 [hep-th]]; M. Cicoli, F. Quevedo and R. Valandro, *JHEP* **1603** (2016) 141 doi:10.1007/JHEP03(2016)141 [arXiv:1512.04558 [hep-th]].
- [30] A. P. Braun, M. Rummel, Y. Sumitomo and R. Valandro, *JHEP* **1512** (2015) 033 doi:10.1007/JHEP12(2015)033 [arXiv:1509.06918 [hep-th]].
- [31] M. Cicoli, K. Dutta and A. Maharana, *JCAP* **1408** (2014) 012 doi:10.1088/1475-7516/2014/08/012 [arXiv:1401.2579 [hep-th]].
- [32] M. Cicoli, I. Garca-Etxebarria, C. Mayrhofer, F. Quevedo, P. Shukla and R. Valandro, arXiv:1706.06128 [hep-th].
- [33] Keck Array, BICEP2 Collaborations: P. A. R. Ade et. al, *Phys. Rev. Lett.* **116**, 031302 (2016). [arXiv:1510.09217]
- [34] Planck Collaboration, R. Adam et al., *Astronomy and Astrophysics* **Volume 594**, (2016) A10
- [35] P. A. R. Ade et al., *Phys. Rev. Lett.* **114** (2015) 101301 [arXiv:1502.00612 [astro-ph.CO]]
- [36] P.F. de Salas et.al. *Phys. Rev. D* **92** no.12, 123534 (2015) doi:10.1103/PhysRevD.92.123534 [arXiv:1511.00672]
- [37] M. Cicoli, J. P. Conlon and F. Quevedo, *Phys. Rev. D* **87** (2013) no.4, 043520 doi:10.1103/PhysRevD.87.043520 [arXiv:1208.3562 [hep-ph]]. T. Higaki and F. Takahashi, *JHEP* **1211** (2012) 125 doi:10.1007/JHEP11(2012)125 [arXiv:1208.3563 [hep-ph]].
- [38] S. Bhattacharya, K. Dutta and A. Maharana, *Phys. Rev. D* **96**, no. 8, 083522 (2017) doi:10.1103/PhysRevD.96.083522 [arXiv:1707.07924 [hep-ph]].
- [39] K. Nakayama, S. Saito, Y. Suwa and J. Yokoyama, *JCAP* **0806**, 020 (2008) doi:10.1088/1475-7516/2008/06/020 [arXiv:0804.1827 [astro-ph]].
- [40] S. Kuroyanagi, C. Gordon, J. Silk and N. Sugiyama, *Phys. Rev. D* **81**, 083524 (2010) Erratum: [*Phys. Rev. D* **82**, 069901 (2010)] doi:10.1103/PhysRevD.82.069901, 10.1103/PhysRevD.81.083524 [arXiv:0912.3683 [astro-ph.CO]].
- [41] L. Aparicio, M. Cicoli, B. Dutta, S. Krippendorff, A. Maharana, F. Muia and F. Quevedo, *JHEP* **1505** (2015) 098 doi:10.1007/JHEP05(2015)098 [arXiv:1502.05672 [hep-ph]]. L. Aparicio, M. Cicoli, B. Dutta, F. Muia and F. Quevedo, *JHEP* **1611** (2016) 038 doi:10.1007/JHEP11(2016)038 [arXiv:1607.00004 [hep-ph]].
- [42] R. H. Cyburt et al., *Rev.Mod.Phys.* **88** (2016) 015004, arXiv:1505.01076 [astro-ph.CO]. N. Sasankan, M. R. Gangopadhyay, G. J. Mathews and M. Kusakabe, *Phys. Rev. D* **95**, 083516 (2017) DOI: 10.1103/PhysRevD.95.083516 arXiv:1607.06858 [astro-ph.CO]. N. Sasankan, M. R. Gangopadhyay, G. J. Mathews and M. Kusakabe, *IJMPE* Vol. 26, No. 7 (2017) 1741007 DOI: 10.1142/S0218301317410075 arXiv:1706.03630 [astro-ph.CO]
- [43] J. J. Blanco-Pillado, D. Buck, E. J. Copeland, M. Gomez-Reino and N. J. Nunes, *JHEP* **1001** (2010) 081 doi:10.1007/JHEP01(2010)081 [arXiv:0906.3711 [hep-th]].
- [44] R. Easther, J. Frazer, H. V. Peiris and L. C. Price, *Phys. Rev. Lett.* **112** (2014) 161302 doi:10.1103/PhysRevLett.112.161302 [arXiv:1312.4035 [astro-ph.CO]].
- [45] P. Cabella, A. Di Marco and G. Pradisi, *Phys. Rev. D* **95** (2017) no.12, 123528 doi:10.1103/PhysRevD.95.123528 [arXiv:1704.03209 [astro-ph.CO]].
- [46] K. D. Lozanov and M. A. Amin, *Phys. Rev. Lett.* **119** (2017) no.6, 061301 doi:10.1103/PhysRevLett.119.061301 [arXiv:1608.01213 [astro-ph.CO]]. K. D. Lozanov and M. A. Amin, arXiv:1710.06851 [astro-ph.CO].